Research Article

Gene therapy with caspase-3 small interfering RNA-nanoparticles is neuroprotective after optic nerve damage

https://doi.org/10.4103/1673-5374.313068

Date of submission: February 7, 2021

Date of decision: February 20, 2021

Date of acceptance: March 1, 2021

Date of web publication: April 23, 2021

Mohamed Tawfik[1, #], Xiwei Zhang[2, #], Lisa Grigartzik[1], Peter Heiduschka[3], Werner Hintz[2], Petra Henrich-Noack[1, 4], Berend van Wachem[2], Bernhard A. Sabel[1, 5, *]

Abstract

Apoptosis, a key mechanism of programmed cell death, is triggered by caspase-3 protein and lowering its levels with gene therapy may rescue cell death after central nervous system damage. We developed a novel, non-viral gene therapy to block caspase-3 gene expression using small interfering RNA (siRNA) delivered by polybutylcyanoacrylate nanoparticles (CaspNPs). *In vitro* CaspNPs significantly blocked caspase-3 protein expression in C6 cells, and when injected intraocularly *in vivo*, CaspNPs lowered retinal capsase-3 immunofluorescence by 57.9% in rats with optic nerve crush. Longitudinal, repeated retinal ganglion cell counts using confocal neuroimaging showed that post-traumatic cell loss after intraocular CaspNPs injection was only 36.1% *versus* 63.4% in lesioned controls. Because non-viral gene therapy with siRNA-nanoparticles can selectively silence caspace-3 gene expression and block apoptosis in post-mitotic neurons, siRNA delivery with nanoparticles may be promising for neuroprotection or restoration of central visual system damage and other neurological disorders. The animal study procedures were approved by the German National Act on the use of experimental animals (Ethic Committee Referat Verbraucherschutz, Veterinärangelegenheiten; Landesverwaltungsamt Sachsen-Anhalt, Halle, Germany, # IMP/G/01-1150/12 and # IMP/G/01-1469/17).

Key Words: apoptosis; brain; caspase-3; drug delivery; gene therapy; *in vivo* confocal neuroimaging; nanoparticles; neurodegeneration; neuroprotection; retina; siRNA

Chinese Library Classification No. R459.9; R364; R774

Introduction

Apoptosis, a programmed cell death, plays a crucial role in development, degeneration, and regeneration in many body organs, especially the brain (Taylor et al., 2008; Fuchs and steller, 2011; Benowitz et al., 2014). Many factors such as aging and trauma can trigger apoptosis, which is initiated by two pathways (intrinsic and extrinsic) that are regulated by different protein families including mitogen activated protein kinases, Bcl-2 and caspases. But the cardinal trigger for apoptosis is caspase-3 (D'Amelio et al., 2012; McIlwain et al., 2015). Because apoptosis in the central nervous system (CNS) can lead to irreversible neurological dysfunctions (Zhang et al., 1999), finding means of gene therapy to reduce or stop caspace-3 synthesis could be a promising approach to slow down or halt neurodegenerative diseases.

We selected the visual system as a model of CNS degeneration to evaluate the possibility of neuroprotection by blocking caspase-3 synthesis with nanoparticle delivery of small interfering RNA (siRNA) in the retina. Because the retina is a CNS tissue, any findings might be applicable to other neuropsychiatric diseases. The loss of retinal ganglion cells (RGCs) with associated optic nerve damage - a cardinal event in glaucoma - can happen suddenly or progress slowly towards irreversible neuronal death and vision loss (Almasieh et al., 2012). We used a preclinical glaucoma model of optic nerve crush (ONC) in adult rats, where RGCs die by apoptosis through cleavage of caspases-3, -8 and -9. Especially elevated caspase-3 levels are problematic, reaching highest levels during a primary wave of RGCs loss, thereafter remaining high while RGCs degenerate (Almasieh et al., 2012; Sánchez-Migallón et al., 2016).

One promising approach to reduce caspace-3 protein levels is gene therapy using viral or non-viral vectors to deliver DNA (e.g. antisense oligonucleotides) or RNA (Kay, 2011; Simonato et al., 2013; Gupta et al., 2018). In recent years, viral vectors have become a popular tool to alter gene expression in the retina to repair deficient genes and achieve neuroprotection with promising results (Hellstrom and Harvey, 2011; Osborne et al., 2018; Ratican et al., 2018; Chiha et al., 2020; Wang et al., 2020). Especially micro RNA or siRNA are powerful means

[1]Institute of Medical Psychology, Otto von Guericke University of Magdeburg, Magdeburg, Germany; [2]Institute of Process Engineering, Otto von Guericke University of Magdeburg, Magdeburg, Germany; [3]Department of Ophthalmology, Münster University Hospital, Münster, Germany; [4]Department of Neurology with Institute of Translational Neurology, Münster University Hospital, Münster, Germany; [5]Center of Behavioral Brain Sciences (CBBS), Magdeburg, Germany

***Correspondence to:** Bernhard A. Sabel, PhD, bernhard.sabel@med.ovgu.de.

https://orcid.org/0000-0002-4472-5543 (Bernhard A. Sabel)

#Both authors contributed equally to this manuscript.

Funding: *MT was funded by the Leistungsorientierte Mittelvergabe (LOM) scholarship offered by the medical faculty of Magdeburg and the Deutscher Akademischer Austauschdienst (DAAD).*

How to cite this article: *Tawfik M, Zhang X, Grigartzik L, Heiduschka P, Hintz W, Henrich-Noack P, van Wachem B, Sabel BA (2021) Gene therapy with caspase-3 small interfering RNA-nanoparticles is neuroprotective after optic nerve damage. Neural Regen Res 16(12):2534-2541.*

to modulate gene expression very specifically, and they were already tested in different diseases such as cancers, infectious, ophthalmologic, or neurological disorders. siRNA can pair with the messenger RNA (mRNA) to either enhance or block protein synthesis (Deng et al., 2014). While the gene of interest is still naïve, the mRNA translation to synthesize proteins is altered (Behlke, 2006; Kim and Rossi, 2007). Because caspase-3 is the key protein of apoptosis, its down-regulation may be achieved by blocking caspase-3 mRNA with its specific caspase-3 siRNA. On the one hand, pure siRNA injections and viral vectors possess certain limitations as well as inherent risks with unique safety challenges which require extensive engineering to satisfy governmental regulations and guidelines (Mullard, 2011; Yin et al., 2014; Hayreh, 2020). On the other hand, pure siRNA cannot be utilized as a therapeutic agent because it has a short life span in serum, being rapidly degraded by ribonucleases, cleared by renal excretion, and non-specifically eliminated by the reticuloendothelial system. Even if siRNA is able to reach its target, it would be rapidly degraded by the highly acidic environment of the endosomes. In addition, pure siRNA could have adverse effects such as unwanted immune reactions or interferon responses (Whitehead et al., 2009; Gavrilov and Saltzmann, 2012). Therefore, employing nanotechnology to protect siRNA from degradation and immune recognition would enhance bioavailability by reducing renal filtration and reticuloendothelial clearance (Setten et al., 2019). To overcome these pharmacokinetic limitations, we developed a siRNA delivery system using non-viral nanoparticle. While nanoparticles have been tested in clinical cancer trials before (Lee et al., 2013) and only one has received marketing approval for rare, inherited liver diseases using lipid nanoparticles (NPs) (Morrison, 2018), none were successful for central nervous system delivery of siRNA where the blood-brain barrier is an obstacle. Yet, biodegradable polymeric NP-systems are able to cross the blood-brain barrier when coated with surfactants such as polysorbate 80, allowing receptor mediated endocytosis in brain capillary endothelial cells (Tosi et al., 2020). Hence, they are suitable delivery systems for the CNS, and, in fact, they were already used in numerous preclinical studies and even for clinical ophthalmic drug delivery (Godse et al., 2016). Furthermore, polymeric NPs can provide a long-term drug release while protecting the encapsulated drug from the surrounding environment (Patel et al., 2012). One kind of biodegradable nanoparticles widely studied for drug delivery across the blood-brain barrier are the poly (butyl cyanoacrylate) nanoparticles (PBCA-NPs) (Kreuter et al., 2003; Tian et al., 2011). Here, by being incorporated or encapsulated inside the nanoparticle, drugs are protected from adverse conditions inside the cells, tissues, or blood, allowing controlled (sustained) release (Voigt et al., 2014; Kolter et al., 2015). Even nucleic acids can be encapsulated in PBCA-NPs using mini-emulsion polymerization methods (Musyanovych et al., 2008), but so far, their use for gene therapy of CNS neurons was only shown *in vitro* (Chung et al., 2013).

To find a means to deliver siRNA to the CNS, we now encapsulated caspase-3 siRNA in polybutylcyanoacrylate nanoparticles (CaspNPs) and tested their feasibility. As we now show for the first time, intraocular injections of CaspNPs can down-regulate caspase-3 and markedly reduce cell death in the retina after optic nerve injury as visualized by repeated and non-invasive *in vivo* confocal neuroimaging (ICON) for more than one month (Sabel et al., 1997; Prilloff et al., 2012). With CaspNPs, we found the first effective siRNA-carrier-system for gene therapy which is able to significantly reduce apoptosis for neural protection and rescue in the CNS.

Materials and Methods

Preparation of PBCA-NPs

Poly (butyl cyanoacrylate) nanoparticles were produced by polymerization in a water-in-oil miniemulsion as previously described (Zhang et al., 2018). Briefly, 4.0 g Migyol 812N (a gift from Cremer Oleo GmbH, Hamburg, Germany) and the surfactant, which was composed of 0.08 g Tween 80 (Sigma-Aldrich, Taufkirchen, Germany) and 0.32 g Span 80 (Carl Roth, Karlsruhe, Germany), were mixed and marked as phase I. Then phase II, 1.2 g phosphate buffered saline (PBS, pH 7.4, 0.1 M) was added dropwise into phase I during stirring for a duration of 30 minutes. The emulsion was then homogenized by ultra-sonication with 50% amplitude for 60 seconds. Thereafter, 100 µL butylcyanoacrylate (Henkel AG & Co. KGaA, Dusseldorf, Germany) monomer was added into the miniemulsion, drop by drop, whilst stirring. After 4 hrs, polymerization was completed, and the nanoparticles were collected by using centrifugation at 8000 × *g* for 5 minutes. The wet pellets were washed with ethanol 3 times and then redispersed in water. For siRNA loading, 5 nmol caspase-3 siRNA (Thermo Fisher, Nidderau, Germany) (Passenger: CCUUACUCGUGAAGAAAUUTT, Guide: AAUUUCUUCACGAGUAAGGTC in the 5′–3′ direction) and non-silencing control RNA (Thermo Fisher) were diluted in phase II and then loaded into the PBCA-NPs. The concentration of these siRNA in the PBCA-NPs was 3.3 µM. Each type of PBCA-NPs (3 µL) was injected intravitreally in all the rat eyes. All steps of the protocol were performed at room temperature (except the homogenization step which was performed on ice to prevent heating of the solution). The same procedure was used for producing blank NPs (PBS) for the *in vivo* study, except that no siRNA was added. Afterwards, NPs were analyzed using a Zetasizer Nano ZS (Malvern Instruments, UK).

Cell culture and protein analysis with western blot

Rat glioma cells (a gift from Max Delbrück Center for Molecular Medicine, Berlin, Germany) were used to investigate caspase-3 siRNA interference *in vitro*. They were cultivated in Ham's F-12K (Kaighn's) Medium (Life Technologies, Darmstadt, Germany), supplemented with 15% horse serum (v/v, Life Technologies), 2.5% fetal bovine serum (v/v, ATCC) and 1% penicillin/streptomycin (v/v, Biochrom AG, Berlin, Germany). All cells were incubated at 37°C in a 5% CO_2 humidified atmosphere.

For western blots, rat glioma cells (C6 cells, a gift from Max Delbrück Center for Molecular Medicine, Berlin, Germany) with a concentration of 20,000/mL were transferred to 6-well-plates 24 hours before treatment. The old medium was replaced by fresh medium containing PBCA-NPs followed by 48 hours incubation. Thereafter, their extracts were collected, and the protein concentrations were measured by Pierce BCA Protein Assay Kit (Thermo Fisher). Subsequently, 25 µg of the protein sample were loaded on SDS-polyacrylamide gel to start the western blot procedure. After electrophoresis and transferring, the caspase-3 protein was imaged after washing with the primary antibody human anti-rat caspase-3 (1:1000, Cat# 6466, Cell Signaling Technology, Frankfurt, Germany; incubated overnight at 4°C) and HRP-conjugated rabbit anti-human IgG (1:1000, Cat# 7074, Cell Signaling Technology; incubated at room temperature for at least 1 hour) consecutively overnight at 4°C. In these experiments, CaspNPs, blank NPs, the mixture of blank NPs and caspase-3 siRNA, caspase-3 siRNA-Ca^{2+} particles, and PBS were used to treat cells using the same protocol, respectively. α-Tubulin protein, which was used as loading control, was detected by using the primary antibody rabbit anti-rat α-tubulin (1:1000, Cat# 2144, Cell Signaling; incubated overnight at 4°C) and HRP-linked secondary antibody (rabbit, 1:1000, Cat# 7074, Cell Signaling Technology; incubated at room temperature for at least 1 hour).

These blotting images were analyzed by ImageJ software (NIH, Rockville, MD, USA). With this software, the images data were

transformed to integrated optical density (IOD) values, which were determined by multiplying the pixel mean grey value of the area by the area of the region of the band. At first, the quantity correlation was calculated from α-tubulin according to Correlation = IOD value for each group/highest IOD value

Thereafter, the IOD values of caspase-3 blots were calculated by the corresponding correlations of the α-tubulin.

***In vivo* study in rats with optic nerve crush**

For all procedures ethical approval was obtained as required by the German National Act on the use of experimental animals (Ethic committee Referat Verbraucherschutz, Veterinärangelegenheiten; Landesverwaltungsamt Sachsen-Anhalt, Halle, Germany, # IMP/G/01-1150/12 and # IMP/G/01-1469/17) adhering to the ARVO (Association for Research in Vision and Ophthalmology, Rockville, MD, USA) statement for the Use of Animals in Ophthalmic and Vision Research in compliance with the ARRIVE guidelines (Animal Research: Reporting of *In Vivo* Experiments). A total of 31 adult, male Lister hooded rats (Crl:LIS Stamm; Charles River, Göttingen, Germany, body weight 280–380 g) were kept on a 12/12-hour light/dark cycle (at 24–26°C and 50–60% humidity). Following shipment, animals were kept at least 3 days for adaptation in group cages and handled for 3 days before starting the experiments. Rats were assigned either to the immunohistochemistry (n = 15) or the ICON experiment (n = 16). The number of animals employed for ICON was as follows: in sub-group A: RGCs survival was tracked for 21 days post ONC (n = 10) whereas in sub-group B survived 35 days post-ONC (n = 6). While CaspNPs were injected in the left eye (n = 15), the right control eye (n = 8) received blank NPs. It turned out that imaging the same rats repeatedly with ICON on a weekly basis is a surgical (anesthesia and imaging) challenge. While all rats were treated and imaged on schedule (treatment: days 0 and 7; imaging: days 0, 7, 14, 21 and 35), we had several drop-outs when image quality was below standard because of spurious imaging artefacts and occasional problems with repetitive anesthesia. In order to reduce the artificial variability introduced by such dropouts, we pooled the cell counting results of the post-acute (days 7–14) and chronic phase (days 21–35). In addition, we calculated the average cell count across all time points (days 7–35) for each rat. However, in the current experiment, we did not recognize any adverse effects: no difference in normal handling, no increased death rate, no abnormal behavior in the eyes or posture compared to control animals.

Optic nerve crush surgery and intraocular injections

Unilateral optic nerve crush surgery was performed using a custom-made forceps (Sautter and Sabel, 1993). Briefly, the rats were anesthetized by intraperitoneal injection of Ketavet (0.75 mL/kg) (ketamine hydrochloride; Zoetis Deutschland GmbH, Berlin, Germany) and Dormitor (0.5 mL/kg) (medetomidine hydrochloride; Orion Corporation, Espoo, Finland). The optic nerve crush was made with calibrated cross-action forceps (KLS Martin Group, Tuttlingen, Germany) applied for 30 seconds at 2–3 mm from the eye with the forceps jaws spaced 0.2 mm apart to produce a moderate crush. Initially, connective tissue was detached from the sclera and a sharp needle (0.8 mm diameter) was used to puncture it, followed by insertion of a Hamilton syringe with blunt cannula for injection into the vitreous. For the *ex vivo* study, 3 µL of CaspNPs were injected into the vitreous body of both sides (n = 3) or, for control purposes, blank NPs (loaded with PBS) (n = 3), non-silencing NPs (n = 3), caspase-3 siRNA-Ca^{2+} particles (n = 3), or PBS (n = 3). For the *in vivo* study, bilateral ONC was performed, and immediately thereafter, the left eye was treated with 3 µL of CaspNPs and the right eye was treated with 3 µL blank NPs suspended in phosphate buffered saline (PBS, pH 7.4, 0.1 M) as control.

Immunofluorescence staining for caspase-3

To image caspace-3 in RGCs, rat eyes were collected 48 hours after the ONC surgery and embedded in paraffin wax. Firstly, both eye balls of the animals were taken out and immersed in 4% formalin. Then, these eyeballs were washed with 4% formalin for 4 hours. Thereafter, the eyeballs were washed successively with 70%, 85%, 2 × 96% and 3 × 100% ethanol solution for 1 hour. Subsequently, they were washed 2 times with RotiHistol for 1 hour and 1.5 hours respectively. Eyeballs were then immersed into liquid paraffin wax for 2 hours. The liquid paraffin wax was refreshed and the eyeball was immersed for another 2 hours, taken out from the oil paraffin, quickly put in an embedding module and covered with new liquid paraffin wax, with subsequent cooling at room temperature for a duration of 3 hours. Finally, the paraffin-embedded eyeballs were stored at 4°C until they were sliced.

The paraffin cubes were cut into slices of 10 µm thickness by a microtome. Then, the slices were put in a water bath at 42°C. The slices were stretched by the surface tension between water and air, and positioned onto the upper surface of Superfrost slides, dried on a hot plate at 50°C for at least 15 minutes until all water was removed. The paraffin sections were stored at 4°C.

Before hydration, the paraffin sections were taken out of the refrigerator and dried again on the hot plate for 10 minutes at 50°C. Hydration was started by washing in a sequence of xylol, 100% ethanol, 96% ethanol, 90% ethanol, 80% ethanol, 70% ethanol solutions, and rinsing with water for 5 minutes each at room temperature. Then, all the slices were immersed in a pre-mixed 0.01 M citrate buffer and heated by steam for 45 minutes, in order to recover antigens in tissues. When the steaming was completed, the samples were cooled down in citrate buffer for 30 minutes at room temperature, and then washed 3 times for 5 minutes each with PBS. The power block solution was added onto all the samples for 6 minutes and subsequently washed 3 times for 5 minutes each with PBS to reduce the background from un-specific immunoreactions. The primary antibodies human anti-rat caspase-3 (1:1000, Cat# 6466, Cell Signaling Technology) were added onto the samples overnight at 4°C (red stain). The antibodies were removed by washing with distilled water on the next day. A secondary antibody conjugated with Alex-fluor 647 (goat anti-human IgG (H+L) Cross-Adsorbed Secondary Antibody, 1:1000, Cat# A21445, Thermo Fisher) was added on the samples for 2 hours in the dark at room temperature. After washing down secondary antibody by PBS three times for 5 minutes each, 2 µg/mL of Hoechst 33342 (Cayman Chemicals, Hamburg, Germany) diluted in water was used to stain the nuclei in the retinal tissues for 6 minutes in the dark (blue stain). Finally, all the samples on slides were closed by coverslips, using Immu-mount (Thermo Fisher).

RGCs

Surgery for RCG labeling

One week before retina baseline imaging, RGCs were selectively labeled by retrograde axonal transport of fluorescent tracer (n = 16 rats). To this end, rats were anaesthetized by intraperitoneal injection of Ketavet/ Dormitor, Ketavet (0.75 mL/kg) (ketamine hydrochloride; Zoetis Deutschland GmbH, Berlin, Germany) and Dormitor (0.5 mL/kg) (medetomidine hydrochloride; Orion Corporation, Espoo, Finland). After drilling openings in the skull, carboxylate-modified microspheres were stereotactically injected (0.04 µm large FluoSpheres; Ex 580/ Em 605, Invitrogen GmbH, Karlsruhe, Germany) into the right and left superior colliculus (coordinates: 6.9 mm posterior to Bregma and –/+1.2 mm lateral from midline) based on its expected stereotaxic coordinates (Paxinos and Watson, 1998). Slow

injections of 0.5 µL were made at each of four different depths below dura (2.5, 3.5, 3.0, 4.0 mm), i.e. 2 µL on each side and allowing 30 seconds for diffusion at each position.

In vivo microscopy with ICON

ICON was carried out 7 days after RGCs labeling as previously described (Sabel et al., 1997; Prilloff et al., 2012). Briefly, rats were anaesthetized by intraperitoneal injection of Ketavet (0.75 mL/kg) and Dormitor (0.5 mL/kg) and for imaging the eyes pupil was dilated with Neosynephrine-POS 2.5% (Arzneimittelherstellung Uniklinik, Magdeburg, Germany). Vidisic optical gel was then applied as an immersion medium for the contact lens to prevent drying of the cornea (Bausch & Lomb, Berlin, Germany). Rats were then positioned under a standard confocal laser scanning microscope (LSM 880, Carl Zeiss AG, Jena, Germany) with a large probe space and a long working distance objective lens. The rat was fixed on the microscope stage with a jaw holder to position the eye directly underneath the objective lens (Plan Neofluar 5x/0.15) after a Hruby style -80 dioptre plan concave lens (KPC-013, Newport GmbH, Darmstadt, Germany) was placed directly onto the cornea, and adjusted in such way that the path of the laser ray focussed on the retina plain. For each rat, we ascertained that images contained enough RGCs so that they could be located again for repeated imaging in the same rat at different time points (7, 14, 21 and 35 days) using blood vessels as landmarks (image size: 2.6 mm^2; image resolution: 800 × 800 pixels, 16-bit) (**Figure 1**).

Ex vivo retina wholemounts

Since the optics resolution of live retina imaging is limited, we also verified cell counts *ex vivo* with whole mount retina preparation. To this end, enucleated eyes (n = 19) were placed post-mortem in Ca^{2+}-free solution (135 mM NaCl, 5 mM NaOH, 2.5 mM KCl, 2 mM $CaCl_2$, 1 mM $MgCl_2$, 10 mM HEPES, 10 mM glucose), the cornea and lenses were removed, and the retina was separated from the pigment epithelium and kept on ice under constant oxygen supply. The tissue was then transferred into a petri dish and mounted on the microscope stage for LSM imaging (objective lens LDC Epiplan-APOchromat 50x/0.5; Image size: 0.24 mm^2; image resolution: 800 × 800 pixels, 16-bit).

RGCs quantitative analysis in vivo and ex vivo

To avoid experimenter bias, RGCs images were coded and counted by two trained and independent observers which were unaware of the animals' group identity. At each imaging time point, the observer counted three separate images and both data sets were then averaged. To ascertain resolution-independent sampling, one observer counted the entire microscopic image (800 × 800 pixels) while the other counted smaller subsections (300 × 300 pixels). Thereafter, RGCs counts between time points were calculated as "percent change over baseline" (%COB) with the equation: [(post-value – pre-value)/pre-value] × 100.

Statistical analysis

Cell counts were summarized as mean ± standard error mean (SEM) and statistically analysed with SPSS Version Statistics 24.0 (IBM Corporation, Armonk, NY, USA). For the western blot and the immunofluorescence' IOD, statistical differences were calculated using one-way analysis of variance (ANOVA) with multiple comparisons using Student-Newman-Keuls test where $P < 0.05$ was considered significant. For ICON, statistical differences between the two groups at each time point were analysed using independent Student's t-test, where $P < 0.05$ was considered significant. Statistical difference between the two groups with all the time points were analysed by a two-way analysis of variance (ANOVA), where $P < 0.001$ was considered significant. *Post hoc* least significant difference test (LSD) was performed to reveal statistical difference between groups.

Results

Characterization of PBCA-NPs

Following fabrication of PBCA-NPs as previously described (Zhang et al., 2018). This revealed a Z-average diameter of blank PBCA-NPs (blank NPs) of 145.3 nm and a zeta-potential of –14.8 mV (n = 3), while CaspNPs' had an average diameter of 217.5 nm and a lower negative zeta-potential (–24.8 mV) (n = 3). Nanoparticles used for ICON experiments of blank PBCA-NPs had a Z-average diameter of 124.08 ± 16.24 and a zeta potential of –11.96 ± 1.67, while CaspNPs' had a diameter of 143.83 ± 26.92 and zeta potential of –9.87 ± 2.74 (n = 3). This was probably due to the negative charge of siRNA, leading to greater electrical repulsion, preventing CaspNPs to aggregate, and thus increasing their diameter. In earlier studies, CaspNPs toxicity was evaluated using MTT assays of C6 glioma cells which showed 0.4% nanoparticles concentrations to be sufficiently safe for our experiments (Zhang et al., 2018).

Caspase-3 silencing by CaspNPs

Western blots probing cleaved caspase-3 expression in C6 cells revealed a significant decrease of caspase-3 protein after the treatment with CaspNPs compared to blank NPs or PBS (**Figure 2A** and **B**). To compare the interference efficiency of CaspNPs with other siRNA variants, a mixture of siRNA and blank NPs was also used as control to transfect C6 cells. Surprisingly, even a simple siRNA-NPs mixture was able to decrease cleaved caspase-3 expression, but this had a large variability when comparing 3 repeats. In addition, another control, a caspase-3 siRNA-Ca^{2+} complex, was tested. Here, siRNA diluted in $CaCl_2$ solution and applied to C6 cells also down-regulated cleaved caspase-3 expression. For more information, please see **Additional Figure 1**.

Silencing caspase-3 expression in retina

To evaluate if CaspNPs can knock-down cleaved caspase-3 expression *in vivo*, we studied caspase-3 immunoreactivity (IR) in retina explants. As expected, ONC led to a higher IR to caspase-3 antibodies in the retina compared to uninjured controls (both groups received PBS as control vehicle), and treatment with CaspNPs injected to eyes of ONC rats markedly reduced caspase-3 IR (**Figure 3A**). This was not seen with blank NPs, caspase-3 siRNA-Ca^{2+} complex and non-silencing NPs (**Figure 3B** and **C**). Thus, only CaspNPs effectively blocked cleaved caspase-3 expression *in vivo*.

***In vivo* quantitative analysis of RGCs counts reveals neuroprotection**

With ICON, it is possible to repeatedly visualize retrogradely labeled RGCs *in vivo* in anaesthetized rats. Using image analysis, we compared the number of retrogradely labeled RGCs in ONC retinae treated either with CaspNPs or blank NPs (**Figure 4A–C**).

At baseline, RGCs cell counts were similar in both groups (CaspNPs: 86.7 ± 4.6, n = 15; blank NP: 77.9 ± 7.1, n = 8), but during the acute post-acute phase following ONC (days 7–14) more RGCs were found in CaspNPs (47.6 ± 5.7, n = 15) compared to blank NPs treated rats (34.1 ± 5.3, n = 8) (n.s.). This difference was more apparent at later survival times in the chronic stage (days 21–35), where the CaspNPs group had significantly more RGCs (55.5 ± 4.6, n = 10) than the blank NPs group (30.2 ± 6.5, n = 5) (P = 0.008). This was also true for the total count across all time points (CaspNPs: 50.9 ± 5.4, n = 15; blank NPs: 32.7 ± 4.6, n = 8; P = 0.039). When expressed as percent change over baseline (%COB), in the post-acute phase, CaspNPs rats lost fewer RGCs (–45.3 ± 4.8%, n = 15) compared to blank NPs (–57.2 ± 5.6%, n = 8), but also here the differences were significant only in the chronic stage. Here, CaspNPs rats showed even a 25% recovery of RGC labeling (–36.1 ± 4.2%, n = 10) while the RGC number in rats treated with blank NP declined even further to –63.4 ± 8% (n = 5, P =

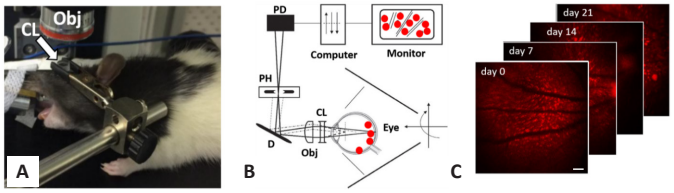

Figure 1 | ***In vivo* confocal neuroimaging (ICON) setup.**
(A) The head of an anaesthetised rat is positioned under the objective (Obj) of a scanning laser microscope (SLO) in a way that the laser beam can be focussed on the retina of the eye. After passing through a contact lens (CL), the laser excites prelabeled RGCs. (B) Cartoon of ICON set-up showing how a photodetector receives photons of fluorescent cell signals via deflector (PD) and pinhole (PH). (C) Red fluorescent cells in the retina then displayed for image analysis at different time points (Sabel et al., 1997). Scale bar: 200 µm.

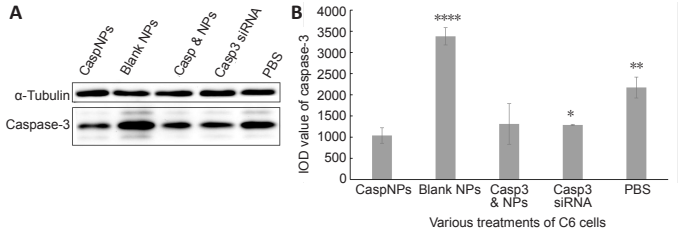

Figure 2 | **Down-regulation of caspase-3 after treatment with CaspNPs.**
(A) Western blot quantification caspase-3 and α-tubulin protein levels in C6 cells treated with CaspNPs, blank NPs, the mixture of caspase-3 siRNA and blank NPs (Casp3 & NPs), Casp3 siRNA, and phosphate buffered saline (PBS). (B) Immunofluorescent signal intensity using integrated optical density (IOD) values (n = 3 per group). Statistical differences were calculated using one-way analysis of variance (ANOVA) with multiple comparisons using Student-Newman-Keuls test. Data are expressed as the mean ± SEM of triplicate tests. *P < 0.05, **P < 0.01, ****P < 0.0001, *vs*. CaspNPs group. NPs: Nanoparticles.

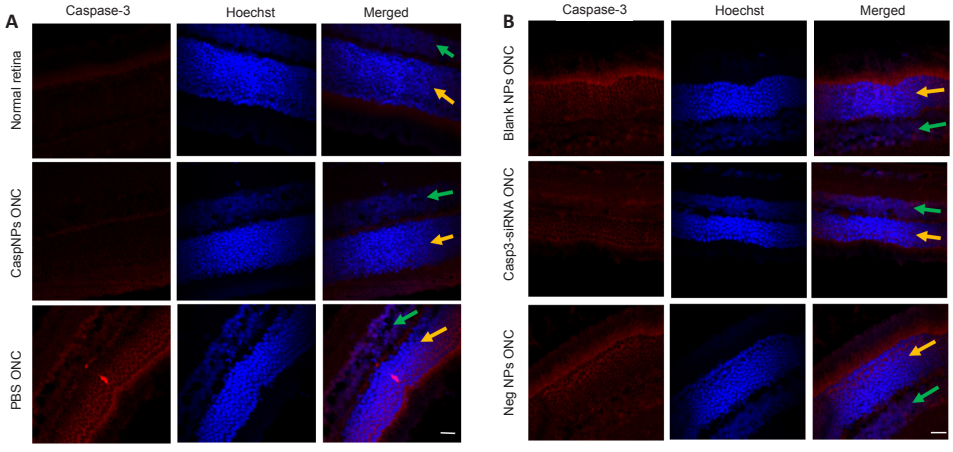

Figure 3 | **Immunofluorescence imaging of caspase-3 in the retina.**
(A) Photomicrogaphs showing caspase-3 antibody retinal labeling (red stain) and retinal cell nuclei by Hoechst 33342 (blue stain). Normal retinae treated with PBS who did not have optic nerve crush (ONC) served as control. ONC induced a high caspase-3 expression in the retina after treatment with PBS when compared with the retina treated with CaspNPs, the caspase-3 protein levels were very low. Scale bar: 20 µm. (B) The effects of blank NPs, caspase-3 siRNA-Ca^{2+} complex (casp3 siRNA) and non-silencing NPs (Neg NPs) after ONC in the retina. However, no obvious down-regulation was observed when retinae with ONC were treated with negative NPs or free caspase-3 siRNA. Scale bar: 20 µm. (A, B) Green arrows indicate the outer nuclear layer and yellow arrows the inner nuclear layers in the retina. (C) Integrated optical density (IOD) values (n = 3 independent animals per group) show the reduction of caspase-3 immunoreactivity by CaspNPs in ONC-damaged retinae with cell numbers which are comparable to the unlesioned (control) retina. In contrast, blank NPs, non-silencing NPs, and free casp3 siRNA did not prevent this loss of immunofluorescence. Statistical differences compared to the normal retina were calculated by one way ANOVA following multiple comparisons using Student-Newman-Keuls test. Data are expressed as means ± SEM. **P < 0.01, *vs*. CaspNPs group. NPs: nanoparticles; PBS: phosphate buffered saline; siRNA: small interfering RNA.

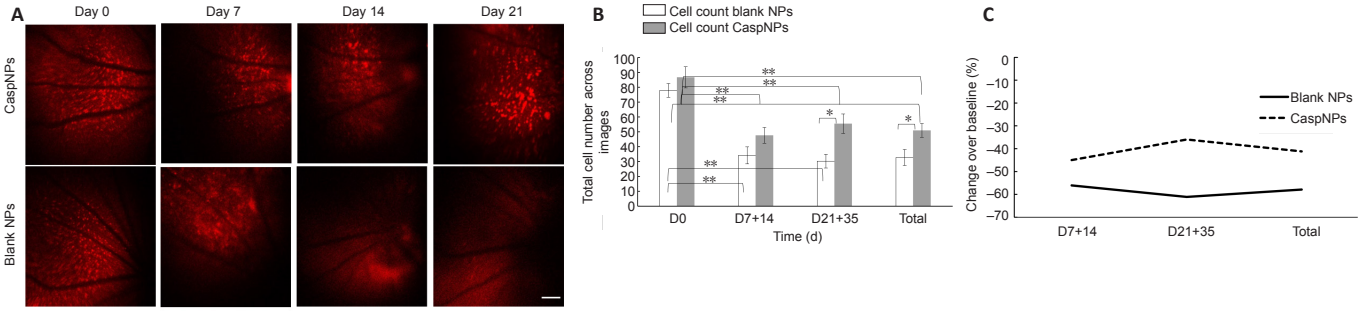

Figure 4 | **Retinal ganglion cell survival effects of CaspNPs *in vivo*.**
(A) Photomicrographs of ICON retinal images on day 0 (baseline) followed by ONC plus 1st treatment; Day 7, ICON plus 2nd treatment; Day 14 and 21 ICON only. Retinal blood vessels visible in black and RGCs retrogradely labeled with 2 µL microspheres (Ex 580/ Em 605) visible in red. The cell density decreased over time. Scale bar: 200 µm. (B) Total RGCs (number/all images) as a function of time: sub-acute stage (D7+D14), chronic stage (D21+35) and across all time points (total) in experimental and control retinae. (D0) CaspNPs and blank NPs, n = 15 and 8 respectively. D7+14: n = 15 and 8 respectively. D21+35: n = 10 and 5 respectively. *P < 0.05 (Student's t-test); **P < 0.001 (two-way analysis of variance); data are expressed as the mean ± SEM. (C) Change over baseline as a function of time. ICON: *In vivo* confocal neuroimaging; NPs: nanoparticles; RGCs: retinal ganglion cells.

0.006). The %COB for the total time was –41.5 ± 4.3% (n = 15) in CaspNPs compared and –58.4 ± 5.3% (n = 8) in blank NP-treated rats (P = 0.028).

RGCs quantitative analysis *ex vivo* imaging

To independently verify the *in vivo* imaging results, in a small sample of sacrificing rats, *ex vivo* whole-mounted retinae were imaged at higher resolution (days 21/35). Here, on day 21, CaspNPs retinae still had more RGCs (49.7 ± 3.6, n = 6) than blank NPs retinae (34.8 ± 3.3) (n = 6). On day 35, the count was (24.0 ± 2.7, n = 4) and (15.9 ± 2.0, n = 3), respectively, confirming the ICON results (**Figure 5A** and **B**). Unlike ICON results, *ex vivo* RGCs counts were not statistically significant which can be explained by the lower signal strength due to laser bleaching after the continuous *in vivo* imaging (days 0, 7, 14, 21, and 35) or because of post-perfusions conditions (such as HEPES buffer, air exposure) which might affect the retinal ganglion cells signal strength and counting results.

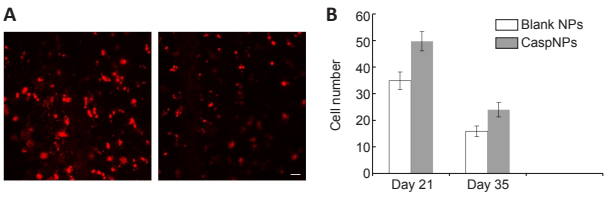

Figure 5 | **Sample of *ex vivo* imaging of retinal ganglion cells survival.**
(A) Representative photomicrographs of retinal ganglions cells as labeled by 2 µL microspheres (Ex 580/ Em 605) in retinal wholemounts post-optic nerve damage. Day 21 shows more RGCs in rats treated with CaspNPs (left) than blank NPs (right). Scale bar: 20 µm. (B) Quantitative analysis of a small sample of RGCs cell counts on day 21 (n = 12) and day 35 (n = 7); however, group comparison was not significant, the average cell count was higher in the CaspNPs group; data are expressed as the mean ± SEM. NPs: Nanoparticles; RGCs: retinal ganglion cells.

Discussion

We demonstrated for the first time that siRNA can be delivered to the CNS with non-viral, polymeric nanoparticles, comprising a novel gene therapy approach to down-regulate caspase-3 expression and protect post-mitotic neurons from apoptosis. This was demonstrated by the novel and highly sensitive non-invasive ICON method (Sabel et al., 1997) which can repeatedly visualize the fate of individual neurons longitudinally for more than one month. Our findings extend prior work of delivering DNA, RNA, or other oligonucleotides by viral vectors (Hellstrom and Harvey, 2011; Chen et al., 2018; Osborne et al., 2018; Ratican et al., 2018; Chiha et al., 2020; Wang et al., 2020), liposomes (Bender et al., 2016), or nanoparticles (Schneider et al., 2008; Duan et al., 2009; Zhang et al., 2014) and even free siRNA has been tested clinically to treat cancer or infections (Lam et al., 2015). But non-viral delivery of siRNA to structures of the CNS has not been achieved: (i) Lipid nanoparticles are rather instable and evidence of reaching CNS neurons is still outstanding (Dowdy, 2017). (ii) Nanoparticles were so far only able to deliver DNA or siRNA to mitotic brain cancer cells where the blood-brain-barrier is damaged (Musyanovych et al., 2008; Duan et al., 2009; Zhang et al., 2014). (iii) The delivery of free siRNA has limited bioavailability and biological effects (Wittrup and Lieberman, 2015). Unlike the present study, prior studies did not succeed to deliver highly specific siRNA to CNS tissues with non-viral delivery methods, and none has achieved neuroprotection.

Our study therefore broadens the potential of NPs to deliver genes to CNS tissues. Delivery to the retina or brain is a fundamental challenge because the blood-retina barrier (which is similar to the blood-brain barrier) is a major hurdle for ophthalmological pharmacology (London et al., 2018). Today, the standard of clinical care to treat retinal and optic nerve diseases is the use of eye drops, or surgery. But intravitreous eye injections are now regularly used in clinical ophthalmology, suggesting that intraocular nanoparticle delivery of siRNA might be a realistic clinical option. According to Stokes' law, intravitreally injected NPs settle onto the inner limiting membranes of the retina within a few hours, allowing a controlled drug release for 21 hours to 7 weeks (Gupta, 2006; Edelhauser et al., 2010). But intravitreal injections of CaspNPs are more feasible than, for example, pure siRNA injections, because nanoparticles reduce or avoid poor cellular uptake and immunogenicity, and their biological half-life is much longer than the current siRNA approaches which last only several minutes to one hour (Layzer et al., 2004; Gavrilov and Saltzmann, 2012). Therefore, nanoparticle formulations can overcome such pharmacokinetic problems and potentially achieve stable gene expression changes (Musyanovych et al., 2008).

Because the retina is CNS tissue, the survival of post-mitotic neurons critically depends on a well-balanced homoeostasis. Our challenge was to identify a nanoparticle design which is both effective and safe. We selected the PBCA-nano-technology proposed by (Kreuter et al., 2003) and (Kolter et al., 2015) who showed their feasibility to cross the blood-brain barrier. Yet, they reported increased cytotoxicity when incubation time or concentration reaches a certain threshold beyond which reactive oxygen species could damage cells. To reduce this cytotoxicity risk, we used water-in-oil mini-emulsions containing only biologically benign Tween 80 and Span 80 as surfactants. Having established safe doses (Zhang et al., 2018), we determined caspase-3 protein levels using western blots of C6 cells and visualized caspase-3 antibodies by IOD of retinal explants.

Surprisingly, survival effects were not only seen with CaspNPs but also with a mixture of blank NPs and free caspase-3 siRNA (caspase-3 & NPs). This suggests that siRNA can form a complex with nanoparticles due to their high surface activity which supports the argument that the NP-surface is a critical parameter for its interaction with biological systems and surface modification is the key determinant for drug delivery (here: for siRNA) (Voigt et al., 2014). We conclude that the PBCA-NPs matrix is not rate limiting for release of incorporated siRNA.

We next checked the silencing effect of CaspNPs *ex vivo* and *in vivo* using a rat model of traumatic optic nerve axonal injury known the induce retrograde cell death of RGCs with delayed, apoptotic cell death (Bien et al., 1999) where caspase-3 is a key triggering signal. Neurotrauma following ONC significantly increases caspase-3 levels in the retina already 2 days post-lesion, but when receiving intravitreal injections of CaspNPs, caspase-3 associated immune-reactivity decreased to near normal levels. Of note, while our NPs lowered caspase-3 immunohistochemistry by almost 60%, in future studies it would be important to determine the levels of activated caspase-2 to gain a better understanding of the activated caspase-3. Moreover, while we report neuroprotection of retinal ganglion cells using the downregulation of caspase-3, there are also other options of neuroprotection such as caspase-2 (Vigneswara and Ahmed, 2016) and caspase-7 (Larner et al., 2005) which, in our case, can still induce the cell death pathway even with blocking caspase-3. Hence, before recommending clinical application of our approach behavioural studies are needed to document the functional significance of our approach.

There are several differences regarding caspase-3 expression between the *in vitro* and *ex vivo* condition. While C6 cell cultures exposure to blank NPs induced a significant increase in caspase-3 expression *in vitro* compared to PBS, this was not

seen *ex vivo*. This suggests PBCA-NPs to be safe for intravitreal application. Furthermore, unlike *in vitro*, intravitreal *in vivo* injections of caspase-3 siRNA alone were not able to knock-down caspase-3 expression. Furthermore, *in vitro* caspase-3 siRNA, at least as a Ca^{2+}-complex, was able to cross the cell membrane and knock-down caspase-3 expression. There are several reasons why *in vitro* and *in vivo* results did not match. The retina and brain have many cell types such as endothelial cells, neurons, rods, cones, glia, and Müller cells. In addition, the *in vivo* (tissue) environment is rather complex because it contains blood vessels and extracellular matrix, with membranes which (for good reasons) limit diffusion of foreign substances, such as siRNA, into nerve tissue. We suppose that especially the inner limiting membrane, separating the retina parenchyma from the vitreous humour, may be an unsurmountable obstacle for passage of free siRNA. Yet, CaspNPs were able to penetrate all retinal layers and knock-down caspase-3 synthesis. Thus, *in vitro* tests are of rather limited value to study NPs drug delivery systems and only *ex vivo* and/or *in vivo* studies in a rodent model deliver the critical information for early-stage drug development.

In conclusion, we succeeded designing a polymeric nanoparticle system, CaspNPs, for the delivery of nucleic acid sequences (here: siRNA) into central nervous system tissue (here: retina). CaspNPs may thus comprise a potentially new gene therapy for glaucoma, a disease which is among the leading causes of blindness, expected to reach a prevalence of > 100 million worldwide by 2040 (Tham et al., 2014).

Glaucoma is characterized by optic nerve damage with subsequent RGCs death due to abnormally high intraocular pressure and/or vascular dysregulation (Flammer et al., 2013), but lowering intraocular pressure with eye drops or surgery does not always stop progression of cell loss (Zhang et al., 2012). Therefore, our new gene therapy approach using CaspNPs might be able to reduce or stop RGCs apoptosis more effectively than the current procedures. In fact, it is even conceivable that CaspNPs, like other PBCA-NPs, may also be suitable for intravenous injections (You et al., 2019). But localized, intraocular injections may be preferable, allowing a lower dose of precious biologics and achieve improved targeting to the retina, thus reducing the probability of systemic adverse events. Nevertheless, the therapeutic potential of CaspNPs in rats does not translate directly to application in patients. Before assessing their clinical value in controlled clinical trials, we need to gain more understanding of the mechanisms of action, pharmacokinetic release profiles *in vitro* or *in vivo*, and efficacy and safety studies of a single intravitreal injection which will help to explore the optimal treatment regimens of treatment dose and duration following intravitreal injections. Last but not least, the neuroprotective effect of encapsulated caspase-2 is worth to study as well, because the inhibition of caspase-2 by modified siRNA can protect 98% of RGCs from apoptosis, 7 days after ONC (Vigneswara et al., 2012) and this protection lasted for at least 30 days.

Our findings have several general implications: first, we learned that nanoparticles can successfully deliver siRNA *in vivo* to CNS neurons, blocking the cardinal trigger for apoptosis, caspase-3 gene expression, remaining biologically active for much longer than one day. Second, caspase-3 siRNA rescues neurons at risk, and thirdly, our *in vivo* gene therapy of post-mitotic neurons is possible without the use of viral vectors. Therefore, gene therapy with siRNA-nanoparticles opens new perspectives for neuroprotection of cell loss in glaucoma and possibly other ophthalmological and neurodegenerative disorders, both of which are on the rise in our aging societies.

Acknowledgments: *We are grateful to Dr. Robert Langer at MIT (Cambridge, USA) for help with editing our manuscript. Susanne Bonifatius (Otto-von-Guericke-University of Magdeburg, Experimental Dermatology) is acknowledged for helping with western blot imaging. Cremer Oleo GmbH & Co. KG kindly provided Migyol 812N. Hanad Farah (Max Delbrück Center for Molecular Medicine in Berlin) provided a C6 cell line and Ying Gao (Otto-von-Guericke-University of Magdeburg, Medical Psychology) helped with the statistical analysis.*

Author contributions: *MT performed the in vivo experiments, including retrograde labelling, ICON, preparation and imaging of wholemount retina and did part of calculation of in vivo cell counting. XZ performed PBCA-NP preparation, western blot and immunofluorescence. LG also performed in vitro and in vivo experiments, including PBCA-NPs preparation and did part of the analysis. PH assisted in intravitreal injection and immunohistochemistry. WH assisted in developing and producing PBCA-NP. PHN designed the research and concept. BAS assisted in designing the experiment. BVW and all other authors have critically contributed to the writing and approved the final manuscript.*

Conflicts of interest: *The authors declare no conflicts of interest.*

Financial support: *MT was funded by the Leistungsorientierte Mittelvergabe (LOM) scholarship offered by the medical faculty of Magdeburg and the Deutscher Akademischer Austauschdienst (DAAD).*

Institutional review board statement: *The animal study procedures were approved by the German National Act on the use of experimental animals (Ethic committee Referat Verbraucherschutz, Veterinärangelegenheiten; Landesverwaltungsamt Sachsen-Anhalt, Halle, Germany, # IMP/G/01-1150/12 and # IMP/G/01-1469/17).*

Copyright license agreement: *The Copyright License Agreement has been signed by all authors before publication.*

Data sharing statement: *Datasets analyzed during the current study are available from the corresponding author on reasonable request.*

Plagiarism check: *Checked twice by iThenticate.*

Peer review: *Externally peer reviewed.*

Additional file:

Additional Figure 1: *α-Tubulin and cleaved caspase-3 protein analysis using western blot.*

References

Almasieh M, Wilson AM, Morquette B, Cueva Vargas JL, Di Polo A (2012) The molecular basis of retinal ganglion cell death in glaucoma. Prog Retin Eye Res 31:152-181.

Behlke MA (2006) Progress towards in vivo use of siRNAs. Mol Ther 13:644-670.

Bender HR, Kane S, Zabel MD (2016) Delivery of therapeutic siRNA to the CNS using cationic and anionic liposomes. J Vis Exp 113:e54106.

Benowitz LI, He Z, Goldberg JL (2017) Reaching the brain: advances in optic nerve regeneration. Exp Neurol 287:365-373.

Bien A, Seidenbecher CI, Böckers TM, Sabel BA, Kreutz MR (1999) Apoptotic versus necrotic characteristics of retinal ganglion cell death after partial optic nerve injury. J Neurotrauma 16:153-163.

Chen YH, Keiser MS, Davidson BL (2018) Viral vectors for gene transfer. Curr Prot Mouse Biol 8:e58.

Chiha W, Bartlett CA, Petratos S, Fitzgerald M, and Harvey AR (2020) Intravitreal application of AAV-BDNF or mutant AAV-CRMP2 protects retinal ganglion cells and stabilizes axons and myelin after partial optic nerve injury. Exp Neurol 326:113167.

Chung CY, Yang JT, Kuo YC (2013) Polybutylcyanoacrylate nanoparticle-mediated neurotrophin-3 gene delivery for differentiating iPS cells into neurons. Biomaterials 34:5562-5570.

D'Amelio M, Sheng M, Cecconi F (2012) Caspase-3 in the central nervous system: beyond apoptosis. Trends Neurosci 35:700-709.

Deng Y, Wang CC, Choy KW, Du Q, Chen J, Wang Q, Li L, Chung TK, Tang T (2014) Therapeutic potentials of gene silencing by RNA interference: principles, challenges, and new strategies. Gene 538:217-227.

Dowdy SF (2017) Overcoming cellular barriers for RNA therapeutics. Nat Biotechnol 35:222.

Duan J, Zhang Y, Chen W, Shen C, Liao M, Pan Y, Wang J, Deng X, Zhao J (2009) Cationic polybutyl cyanoacrylate nanoparticles for DNA delivery. J Biomed Biotechnol 2009:149254.

Edelhauser HF, Rowe-Rendleman CL, Robinson MR, Dawson DG, Chader GJ, Grossniklaus HE, Rittenhouse KD, Wilson CG, Weber DA, Kuppermann BD, Csaky KG (2010) Ophthalmic drug delivery systems for the treatment of retinal diseases: basic research to clinical applications. Invest Opthalmol Vis Sci 51:5403-5420.
Flammer J, Konieczka K, Flammer AJ (2013) The primary vascular dysregulation syndrome: implications for eye diseases. EPMA J 4:14.
Fuchs Y, Steller H (2011) Programmed cell death in animal development and disease. Cell 147:742-758.
Gavrilov K, Saltzman WM (2012) Therapeutic siRNA: principles, challenges, and strategies. Yale J Biol Med 85:187-200.
Godse R, Singh K, Shrivastava A, Shinde U (2016) Polymeric nanoparticulate systems: A potential approach for ocular drug delivery. In Nano-biomaterials for ophthalmic drug delivery (Pathak Y, Sutariya V, Hirani AA, eds), pp351-387. Cham: Springer Int Pub.
Gupta RB (2006) Fundamentals of drug nanoparticles in nanoparticle technology for drug delivery (Gupta RB, Kompella UB, eds), pp1-20. New York: Taylor & Francis Group.
Gupta S, Fink MK, Ghosh A, Tripathi R, Sinha PR, Sharma A, Hesemann NP, Chaurasia SS, Giuliano EA, Mohan RR (2018) Novel combination BMP7 and HGF gene therapy instigates selective myofibroblast apoptosis and reduces corneal haze in vivo. Invest Opthalmol Vis Sci 59:1045-1057.
Hayreh SS (2020) Controversies on neuroprotection therapy in non-arteritic anterior ischaemic optic neuropathy. Br J Ophthalmol 104:153-156.
Hellstrom M, Harvey AR (2011) Retinal ganglion cell gene therapy and visual system repair. Curr Gene Ther 11:116-131.
Kay MA (2011) State-of-the-art gene-based therapies: the road ahead. Nat Rev Genet 12:316-328.
Kim DH, Rossi JJ (2007) Strategies for silencing human disease using RNA interference. Nat Rev Genet 8:173-184.
Kolter M, Ott M, Hauer C, Reimold I, Fricker G (2015) Nanotoxicity of poly (n-butylcyano-acrylate) nanoparticles at the blood–brain barrier, in human whole blood and in vivo. J Control Release 197:165-179.
Kreuter J, Ramge P, Petrov V, Hamm S, Gelperina SE, Engelhardt B, Alyautdin R, Von Briesen H, Begley DJ (2003) Direct evidence that polysorbate-80-coated poly (butylcyanoacrylate) nanoparticles deliver drugs to the CNS via specific mechanisms requiring prior binding of drug to the nanoparticles. Pharm Res 20:409-416.
Lam JK, Chow MY, Zhang Y, Leung SW (2015) siRNA versus miRNA as therapeutics for gene silencing. Mol Ther Nucleic Acids 4:e252.
Larner SF, Hayes RL, McKinsey DM, Pike BR, Wang KK (2005) Caspase 7: increased expression and activation after traumatic brain injury in rats. J Neurochem 94:97-108.
Layzer JM, McCaffrey AP, Tanner AK, Huang ZA, Kay MA, Sullenger BA (2004) In vivo activity of nuclease-resistant siRNAs. RNA 10:766-771.
Lee JM, Yoon TJ, Cho YS (2013) Recent developments in nanoparticle-based siRNA delivery for cancer therapy. Biomed Res Int 2013:782041.
London A, Benhar I, Schwartz M (2013) The retina as a window to the brain—from eye research to CNS disorders. Nat Rev Neurol 9:44.
McIlwain DR, Berger T, Mak TW (2013) Caspase functions in cell death and disease. Csh Perspect Biol 5:a008656.
Morrison C (2018) Alnylam prepares to land first RNAi drug approval. Nat Rev Drug Discov 17:156-157.
Mullard A (2011) Gene therapies advance towards finish line. Nat Rev Drug Discov 10:719-720.
Musyanovych A, Landfester K (2008) Synthesis of poly (butylcyanoacrylate) nanocapsules by interfacial polymerization in miniemulsions for the delivery of DNA molecules. In: Surface and interfacial forces-from fundamentals to applications (Auernhammer G, Butt HJ, Vollmer D, eds), pp120-127. Heidelberg: Springer Int Pub.
Osborne A, Khatib TZ, Songra L, Barber AC, Hall K, Kong GY, Widdowson PS, Martin, KR (2018) Neuroprotection of retinal ganglion cells by a novel gene therapy construct that achieves sustained enhancement of brain-derived neurotrophic factor/tropomyosin-related kinase receptor-B signaling. Cell Death Dis 9:1-18.
Patel T, Zhou J, Piepmeier JM, Saltzman WM (2012) Polymeric nanoparticles for drug delivery to the central nervous system. Adv Drug deliv Rev 64:701-705.
Paxinos G, Watson C (1998) The rat brain in stereotaxic coordinates, 4th ed. New York: Academic Press.
Prilloff S, Henrich-Noack P, Sabel BA (2012) Recovery of axonal transport after partial optic nerve damage is associated with secondary retinal ganglion cell death in vivo. Invest Opthalmol Vis Sci 53:1460-1466.
Ratican SE, Osborne A, Martin KR (2018) Progress in gene therapy to prevent retinal ganglion cell loss in glaucoma and Leber's hereditary optic neuropathy. Neural Plast 2018:7108948.
Sabel BA, Engelmann R, Humphrey MF (1997) In vivo confocal neuroimaging (ICON) of CNS neurons. Nat Med 3:244-247.
Sánchez-Migallón MC, Valiente-Soriano FJ, Nadal-Nicolás FM, Vidal-Sanz M, Agudo-Barriuso M (2016) Apoptotic retinal ganglion cell death after optic nerve transection or crush in mice: delayed RGC loss with BDNF or a caspase 3 inhibitor. Invest Opthalmol Vis Sci 57:81-93.
Sautter J, Sabel BA (1993) Recovery of brightness discrimination in adult rats despite progressive loss of retrogradely labelled retinal ganglion cells after controlled optic nerve crush. Eur J Neurosci 5:680-690.
Schneider T, Becker A, Ringe K, Reinhold A, Firsching R, Sabel BA (2008) Brain tumor therapy by combined vaccination and antisense oligonucleotide delivery with nanoparticles. J Neuroimmunol 195(1-2):21-27.
Setten RL, Rossi JJ, Han SP (2019) The current state and future directions of RNAi-based therapeutics. Nat Rev Drug Discov 18:421-446.
Simonato M, Bennett J, Boulis NM, Castro MG, Fink DJ, Goins WF, Gray SJ, Lowenstein PR, Vandenberghe LH, Wilson TJ, Wolfe JH, Glorioso JC (2013) Progress in gene therapy for neurological disorders. Nat Rev Neurol 9:277-291.
Taylor RC, Cullen SP, Martin SJ (2008) Apoptosis: controlled demolition at the cellular level. Nat Rev Mol Cell Biol 9:231-241.
Tham YC, Li X, Wong TY, Quigley HA, Aung T, Cheng CY (2014) Global prevalence of glaucoma and projections of glaucoma burden through 2040: a systematic review and meta-analysis. J Ophthalmol 121:2081-2090.
Tian XH, Lin XN, Wei F, Feng W, Huang ZC, Wang P, Ren L, Diao Y (2011) Enhanced brain targeting of temozolomide in polysorbate-80 coated polybutylcyanoacrylate nanoparticles. Int J Nanomedicine 6:445-452.
Tosi G, Duskey JT, Kreuter J (2020) Nanoparticles as carriers for drug delivery of macromolecules across the blood-brain barrier. Expert Opin Drug Deliv 17:23-32.
Vigneswara V, Berry M, Logan A, Ahmed Z (2012) Pharmacological inhibition of caspase-2 protects axotomised retinal ganglion cells from apoptosis in adult rats. PLoS One 7:53473.
Vigneswara V, Ahmed Z (2016) Long-term neuroprotection of retinal ganglion cells by inhibiting caspase-2. Cell Death Discov 2:16044.
Voigt N, Henrich-Noack P, Kockentiedt S, Hintz W, Tomas J, Sabel BA (2014) Surfactants, not size or zeta-potential influence blood-brain barrier passage of polymeric nanoparticles. Eur J Pharm Biopharm 87:19-29.
Wang Q, Zhuang P, Huang H, Li L, Liu L, Webber HC, Dalal R, Siew L, Fligor CM, Chang KC, Nahmou M (2020) Mouse gamma-synuclein promoter-mediated gene expression and editing in mammalian retinal ganglion cells. J Neurosci 40:3896-3914.
Whitehead KA, Langer R, Anderson DG (2009) Knocking down barriers: advances in siRNA delivery. Nat Rev Drug Discov 8:129-138.
Wittrup A, Lieberman J (2015) Knocking down disease: a progress report on siRNA therapeutics. Nat Rev Gen 16:543-552.
Yin H, Kanasty RL, Eltoukhy AA, Vegas AJ, Dorkin JR, Anderson DG (2014) Non-viral vectors for gene-based therapy. Nat Rev Genet 15:541-555.
You Q, Sokolov M, Grigartzik L, Hintz W, van Wachem BG, Henrich-Noack P, Sabel BA (2019) How nanoparticle physicochemical parameters affect drug delivery to cells in the retina via systemic interactions. Mol Pharm 16:5068-5075.
Zhang C, Raghupathi R, Saatman KE, LaPlaca MC, McIntosh TK (1999) Regional and temporal alterations in DNA fragmentation factor (DFF)-like proteins following experimental brain trauma in the rat. J Neurochem 73:1650-1659.
Zhang J, Li X, Huang L (2014) Non-viral nanocarriers for siRNA delivery in breast cancer. J Control Release 190:440-450.
Zhang K, Zhang L, Weinreb RN (2012) Ophthalmic drug discovery: novel targets and mechanisms for retinal diseases and glaucoma. Nat Rev Drug Discov 11:541-559.
Zhang X, Zhang E, Grigartzik L, Henrich-Noack P, Hintz W, Sabel BA (2018) Anti-apoptosis function of PBCA nanoparticles containing caspase-3 siRNA for neuronal protection. Chem Ing Tech 90:451-455.

C-Editors: Zhao M, Li CH; T-Editor: Jia Y

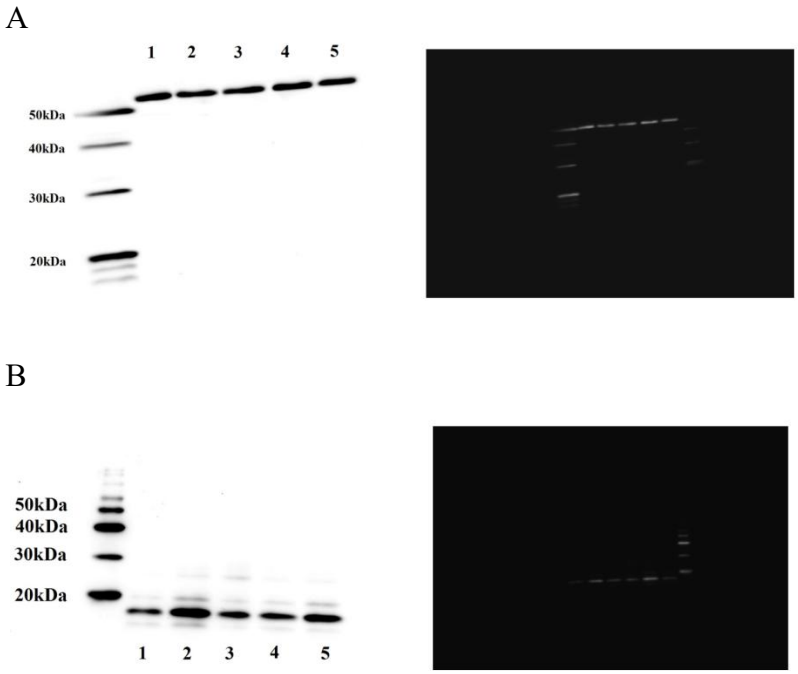

Additional Figures 1 α-Tubulin and cleaved caspase-3 protein analysis using western blot.

(A) α Tubulin. (B) Cleaved caspase-3. 1: CaspNPs; 2: blank NPs; 3: Casp3 and NPs; 4: Casp3 siRNA; 5: PBS. NPs: nanoparticles; PBS: phosphate buffered saline.